

Modal Dynamic Analysis of a Mechanism with Deformable Elements from an Oil Pump Unit Structure

N. Dumitru, S. Dumitru, C. Copilusi, N. Ploscaru

Abstract—On this research, experimental analyses have been performed in order to determine the oil pump mechanism dynamics and stability from an oil unit mechanical structure. The experimental tests were focused on the vibrations which occur inside of the rod element during functionality of the oil pump unit. The oil pump mechanism dynamic parameters were measured and also determined through numerical computations. Entire research is based on the oil pump unit mechanical system virtual prototyping. For a complete analysis of the mechanism, the frequency dynamic response was identified, mainly for the mechanism driven element, based on two methods: processing and virtual simulations with MSC Adams aid and experimental analysis. In fact, through this research, a complete methodology is presented where numerical simulations of a mechanism with deformed elements are developed on a dynamic mode and these can be correlated with experimental tests.

Keywords—Modal dynamic analysis, oil pump, vibrations, flexible elements, frequency response.

I. INTRODUCTION

NOWADAYS artificial pumping systems have the highest operating efficiency of all known generation systems. The oil pumping units design principles and analyses uses rough formulas and procedures based on analytical approaches of conventional oil/gas fields as in [1] and [2]. As regarding the design of these systems, in the specialty literature there is a large number of papers where potential behavior models of the rod pumping systems elements are analyzed. Thus, by taking into account the research developed in [3], [4], based on the linear transformation theory and vector operations, a method of beam pumping unit explicit analysis was carried out, where the difficulties of the quadratic equations method were solved and also the trigonometric functions method was used. In this research there were determined the kinematics and torque factor in the central bearing for three types of beams. These were possible by taking into account the power conservation law and the impact of this avoids the complex computation of the force supported by each beam. Another research, which deals with a calculation method for pumping rod system design, was presented in [5], [6], where the mathematical

model of this was calculated based on kinematic and dynamic analyses of the pumping mechanical system. In this case, the pumping rod loads were determined by considering only the static and inertial loads. In this case, the driving torque was determined based on empirical formulas and correction factors. Also the rod form was considered as polished one for linking the external system located on the ground. This allowed the researchers from the American Petroleum Institute to establish the critical components of this element by taking into account the friction and dynamic loads.

In case of the experimental researches, it is well known that these oil pumping units work in critical conditions and it is very hard to insert in underground measuring sensors. Therefore, for performing a dynamic analysis onto the oil pumping rod, dynamic force sensors can be introduced onto polished element in order to determine the loads and use these as inputs for mathematical models. With this, by considering the rod primary dumping and elasticity parameters, the dynamic behavior of this element can be determined at various well depths. Dynamic models used for numerical computations, were proposed in [7]-[12] and these are especially created for polished rod systems including coupled ordinary differential equations and damped wave equation variations. These models were designed based on the idea that the models should be reliable enough for facilitating a good diagnosis and analysis of the oil pumping unit components.

Based on the actual study on this domain, this research is organized as follows: A state of the art regarding some dynamic models has been analyzed in order to establish the starting premises of this research. Section II represents a general description of the modal-dynamic analysis especially dedicated on the desired oil pumping unit, which gives important input data for virtual simulations performed onto MSC ADAMS software. In Section III, the vibration results for the flexible rod were processed and compared with the ones obtained experimentally, which were described in Section IV. The research ends with important conclusions which regard the dynamic behavior of the rod element from oil pumping units' structures.

II. MECHANISM MODAL-DYNAMIC ANALYSIS

The mechanism modal dynamic analysis starts from a kinematic analysis of the proposed pumping system mechanism. Important results used from this analysis were considered as input data for the proposed research. Thus, these results were published in [13] and for identifying the work

N. Dumitru is with Faculty of Mechanics, University of Craiova. Calea Bucuresti street no. 113. Romania (corresponding author to provide phone: +40747222771, e-mail: nicolae_dtru@yahoo.com).

S. Dumitru is with Faculty of Automation and Computers, University of Craiova. Decebal no. 107. Romania (e-mail: sorindumitru83@yahoo.com).

C. Copilusi and N. Ploscaru are with Faculty of Mechanics, University of Craiova. Calea Bucuresti street no. 113. Romania (e-mail: cristache03@yahoo.co.uk, ploscarunicolae@yahoo.com).

principle of the mechanism, a kinematic scheme is shown in Fig. 1.

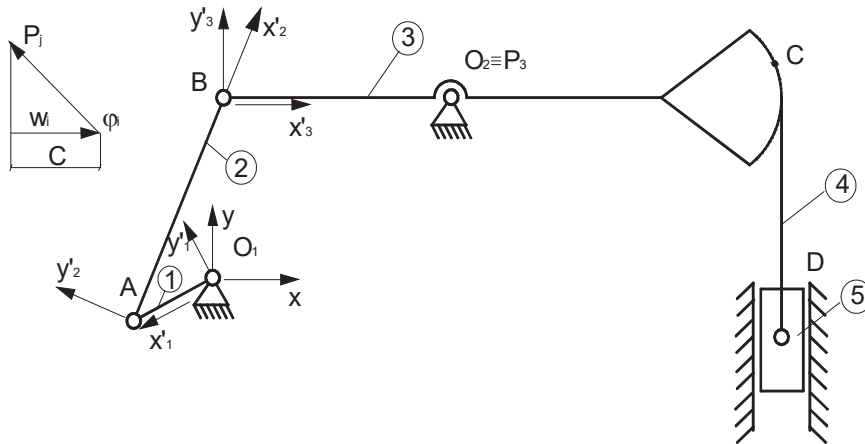


Fig. 1 Kinematic scheme of the pumping unit mechanism

Based on this kinematic scheme and also onto CAD drawings of an oil pumping unit, a virtual model has been designed and this is represented in Fig. 2.

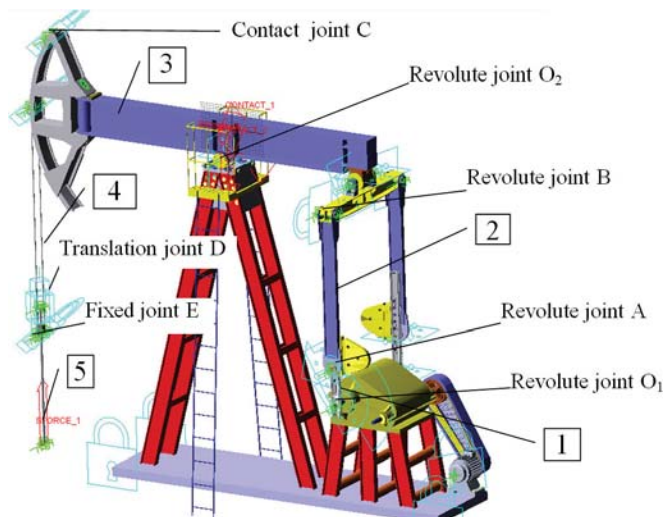


Fig. 2 Oil pumping unit virtual model with joints and elements identification

The CAD model consists of actuation unit (motor- gearbox-belt transmission) and its pumping mechanism. This mechanism was designed in accordance with kinematic scheme from Fig. 1 and by taking into account this scheme, onto the virtual model; the following elements can be identified: Motor element, connecting rod, walking beam, polished rod, and elastic element. This model was imported onto MSC ADAMS software environment, by creating a special interface and a modal dynamic analysis was performed. Generally, this analysis consists of two stages: natural frequencies evaluation and proper vibration modes; an elasto-dynamic analysis.

The mathematical model which lays in the background of this dynamic analysis of a mechanism with a flexible element

or deformable one, is created based on Lagrange formalism, by taking into account the following considerations:

- The generalized coordinates vector for both components namely position and orientation of the mobile reference system is fixed on the flexible element and modal coordinates;
- The position vector of an arbitrary point from the studied element has three components, respectively the position vector of the mobile reference coordinate system origin according with the fixed one, the position vector of a point depends on a mobile reference system and translational deformation vector, which was considered the one from the undeformed position to the deformed one;
- The translational deformation vector will be obtained as a linear combination between modal matrix and modal coordinates (where the modal matrix part will be considered and this corresponds to the translation mobility degrees of freedom of the interest point or node).

The mathematical expressions which define a flexible body motion are obtained by differentiating the Lagrange equations as:

$$\frac{d}{dt} \left(\frac{\partial L}{\partial \dot{\xi}} \right) - \frac{\partial L}{\partial \xi} + \frac{\partial F}{\partial \dot{\xi}} + \left[\frac{\partial \Psi}{\partial \xi} \right]^{-1} \lambda - Q = 0 \quad (1)$$

$$\Psi = 0$$

where: L is the Lagrange form, defined by:

$$L = T - V, \quad (2)$$

“ T ” and “ V ” represent the kinetic and potential energies; “ F ” is the energy dissipation function; “ Ψ ” is the constraints equations; “ λ ” is Lagrange multipliers for constraints; “ ξ ” is the generalized coordinates defined by (3).

The generalized coordinates of a flexible body are:

$$\xi = \{x \ y \ z \ \psi \ \theta \ \varphi \ q_i, (i=1...M)\}^T = \{x \ \psi \ q\}^T \quad (3)$$

From Fig. 2, the flexible element is no. 5, and the procedure for transforming this from a solid rigid body to a deformable one was based on finite element method. The connection between the flexible element no.5 and the polished rod is modeled through a fixed joint (F) and a translational joint (G).

After virtual simulations, for testing the mechanism functionality, a snapshot was taken and presented on Fig. 3, for observing the steel cable behavior (this is equivalent to element no. 5).

A. Modal Analysis

The modal analysis is carried out for determine the natural frequencies and vibration proper modes of the analyzed elements, when these are considered flexible. In this case, the flexible element is the one which connects the walking beam onto polished rod. Also the proper vibration modes of the flexible elements were determined and a snapshot of a proper vibration mode no. 7 is shown in Figs. 4 and 5.

B. Dynamic Analysis

For the pumping mechanism dynamic analysis, it is needed to have some input data. The input data are the following: mechanism geometry obtained on parameterized solid models; material and inertia characteristics; force variation law depending on time which actuate on the polished rod. This force was obtained experimentally and a picture of the sensors placed on this is shown in Fig. 6, and its variation is represented on Fig. 7. Another important parameter, which was determined experimentally, is the walking beam angular variation, namely „ φ_3 ”. This is shown in Fig. 8.



Fig. 3 A snapshots during the oil pumping mechanism kinematic functionality

model_1 Flex Body=PART_9_flex Mode=7 (5.373697 Hz)

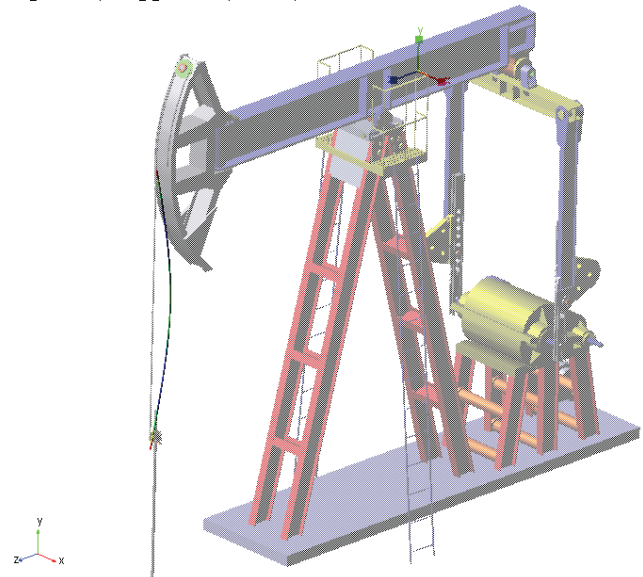


Fig. 4 Flexible element deformation for the proper vibration mode no. 7

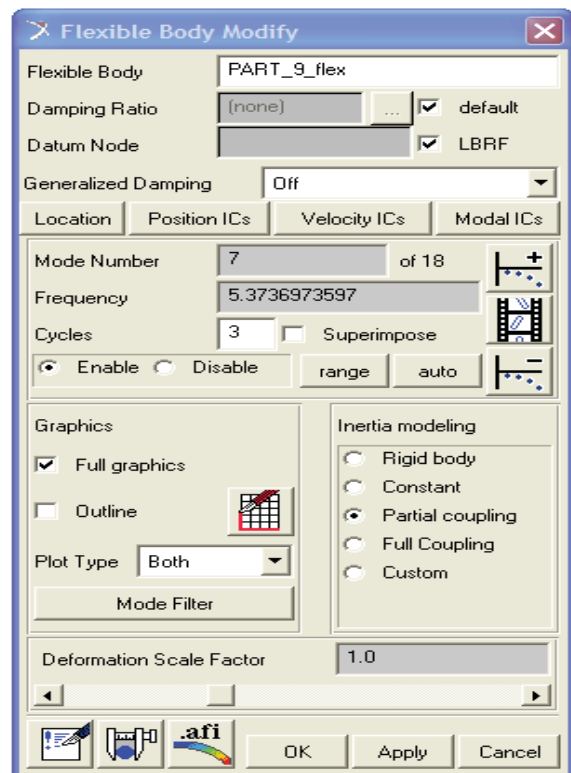


Fig. 5 Flexible element deformation information window for the proper vibration mode no. 7

The mechanism dynamic response was studied theoretically and also experimentally on a time interval from 0 to 8.66 seconds. Through virtual simulations performed onto MSC ADAMS software environment, the response function of the actuation torque was identified in case of the motion actuation joint which was “A” joint. This has the following expression:

$$M_m = M_0 * \left(\frac{1 - WZ(\text{MARKER_55}, \text{MARKER_56}, \text{MARKER_56}) / \omega_0}{\omega_0} \right) \quad (4)$$

where: “Mm” is the drive torque; “M0” represents the initial torque; “ω0” is initial angular speed; “WZ” represents an angular speed resulted in the motion joint.

On a first stage, the dynamic analysis was performed without taking into account the stiffness force from the polished rod. There were identified through virtual simulations the angular speed variation law and torque of the drive element depending on time. This analysis was performed on a set of 5 cycles and the obtained results are shown on diagrams from Figs. 9 and 10.

By analyzing Figs. 9 and 10, it can be remarked that the simulated mechanism has a cyclic functionality for both parameters.

In the second stage, a dynamic analysis was performed by taking into account the stiffness force from the polished rod of the oil pumping mechanism. This was simulated according with the oil pump reality imposed tasks on several cycles. During simulations, the correspondence between reference systems from numerical simulations was kept with the ones from experimental tests.



Fig. 6 Accelerometer sensor placed on the oil pumping unit polished rod

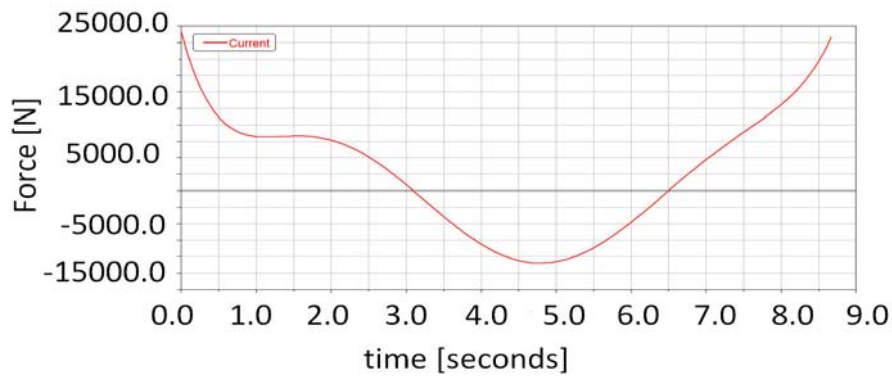


Fig. 7 Force variation law of the oil pumping unit polished rod

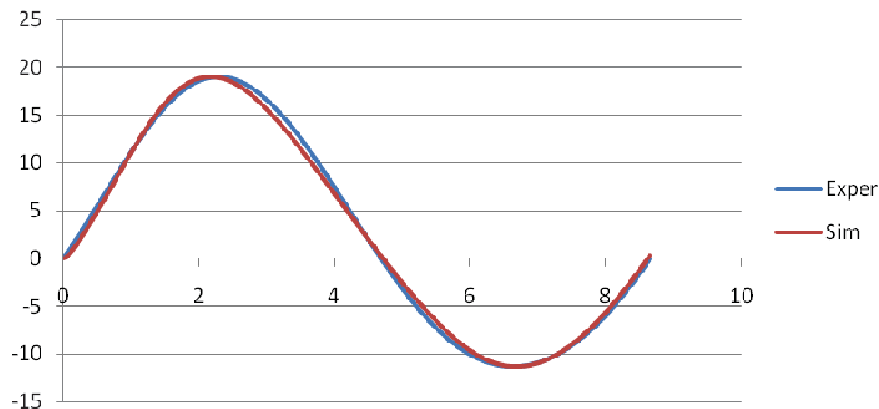


Fig. 8 Walking beam angular variation law of φ₃[degrees] vs. time [seconds]

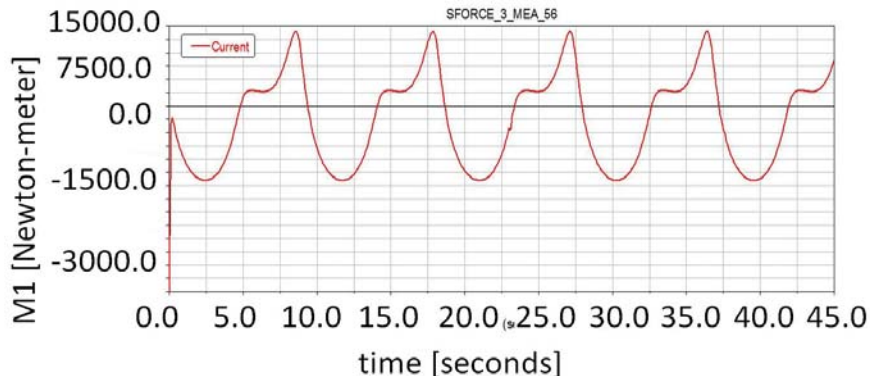


Fig. 9 Torque variation diagram on a 5 cycles vs. time

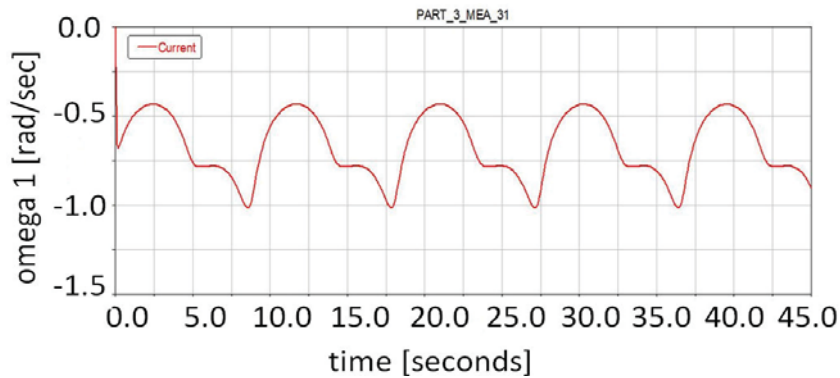


Fig. 10 Angular speed variation diagram on a 5 cycles vs. time

The oil pump mechanism dynamic answer established through modal dynamic analysis was validated with the one obtained on experimental tests. As a comparison element, for this it was considered „φ3” term. This was measured during experimental analysis but also processed through numerical

simulations as it can be seen in Fig. 8. Based on this assurance, other parameter will be analyzed such as kinematic parameters of the element no. 4, namely center of mass when this element was considered as deformable solid. The location of the center of mass was given by the flexible element position marker which is shown in Fig. 11.

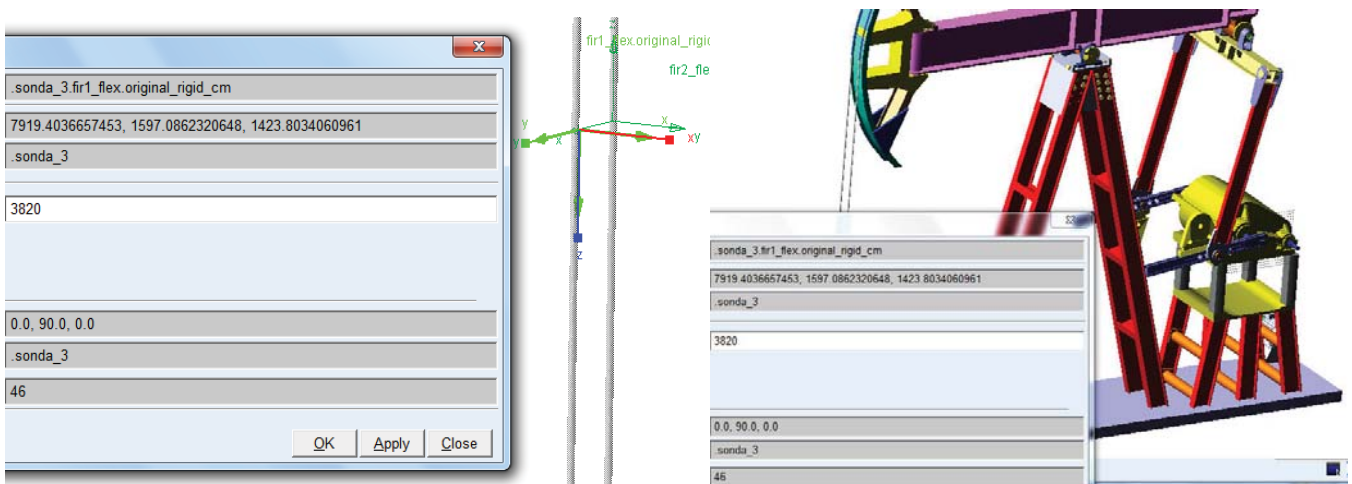


Fig. 11 Marker for center of mass position identification on the analyzed mechanism

For the situation when the oil pumping mechanism works on many cycles (11 cycles), when the initial torque and initial speed will be modified in time, the actuating torque was defined by the following motion law:

$$M_m = 3000000 * \begin{pmatrix} 1 - WZ(\text{MARKER_55}, \\ \text{MARKER_56}, \\ \text{MARKER_56}/0.78 \end{pmatrix} \quad (5)$$

The results obtained are in Figs. 12-15.

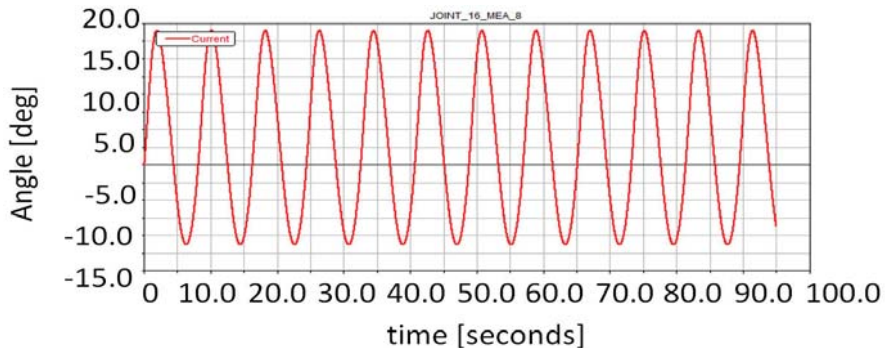


Fig. 12 Walking beam angle variation law φ_3 vs. time

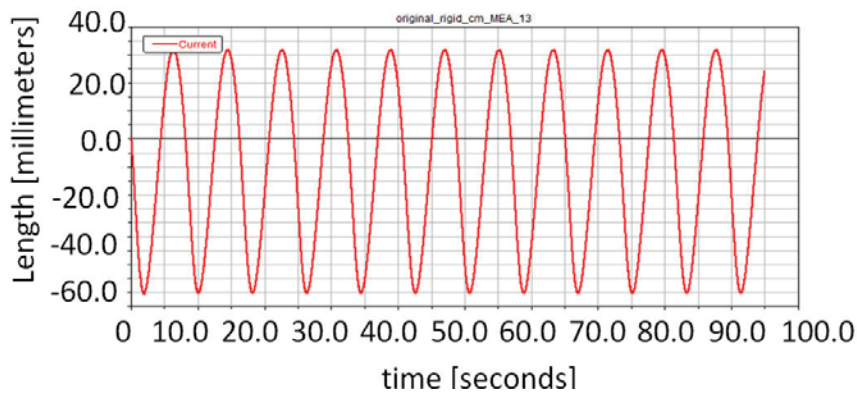


Fig. 13 Translational deformation of the marker position attached on the cable mass center on x-axis vs. time

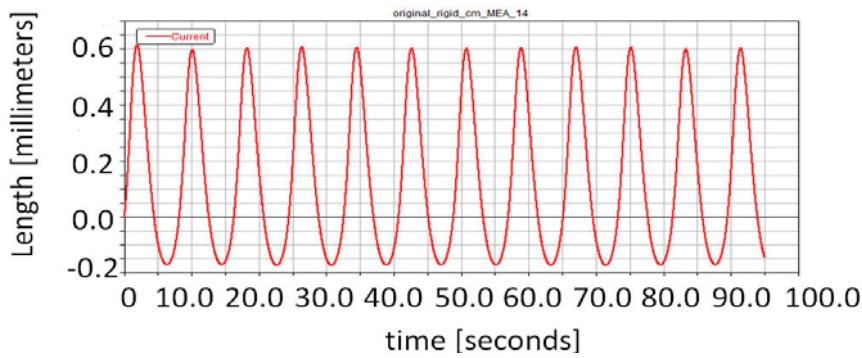


Fig. 14 Translational deformation of the marker position attached on the cable mass center on y-axis vs. time

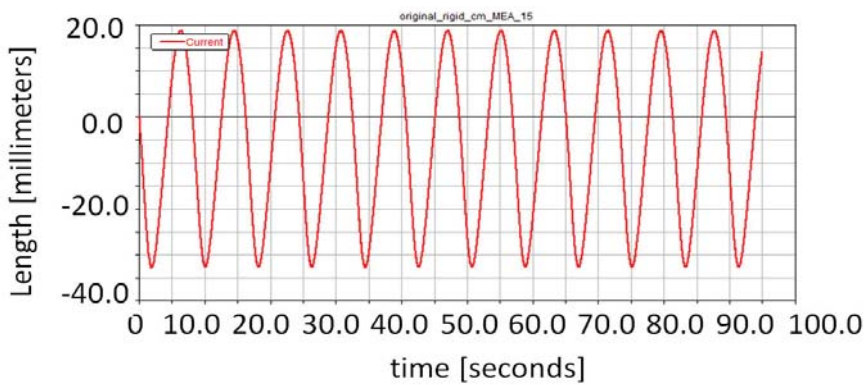


Fig. 15 Translational deformation of the marker position attached on the cable mass center on z-axis vs. time

In Fig. 16, some snapshots during oil pump mechanism virtual simulations are presented.

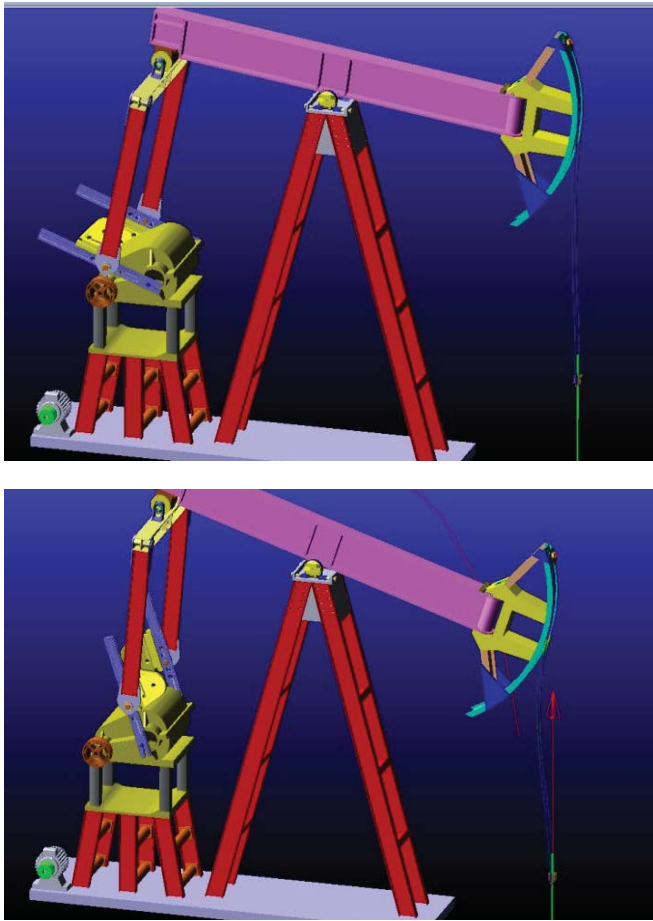


Fig. 16 Snapshots during oil pump mechanism virtual simulations

For dynamic analysis numerical processing, the following input data were necessary: a geometric modeling with solids in a parameterized mode; material and inertia properties; stiffness force variation law from the polished rod established

on experimental analysis. In this case, a procedure under MSC ADAMS environment was established in order to identify the actuating torque variation law. When the oil pump mechanism works under specific tasks, a rotation angle of the walking beam was taken as kinematic reference parameter. By comparing the angle values obtained through virtual simulations with the ones obtained experimentally it can be observed a small error of 3%, which is low enough.

The aim of obtaining the plots from Figs. 12-15 was to analyze the oil pump mechanism working stability at stiffness force variations on the polished rod, respectively at different motion torque values.

III. VIBRATION ANALYSIS OF THE FLEXIBLE ROD ELEMENT

The vibration analysis of the flexible rod element is represented by an elasto-dynamic mechanism analysis, especially the evaluation of the dynamic answer created by vibrations of the mechanism terminal elements. In this case, these elements are represented by the polished rod and the flexible element, which are analyzed with the aid of MSC ADAMS software. For this, it was pursued the following steps:

1. For the imported model onto MSC Adams software environment, there were defined the actuators and the output channels in case of vibration analysis;
2. Frequency domain will be defined for analyzing the free vibrations and also forced ones.
3. In case of free vibrations, there will be studied the frequencies and proper vibrating modes and for the forced ones there will be analyzed the transfer functions, frequency response and participation factors on each degree of freedom, respectively on each vibrating mode.

The actuator role is to generate input forces, displacements, speeds and accelerations in order to produce vibrations inside of the analyzed mechanical system.

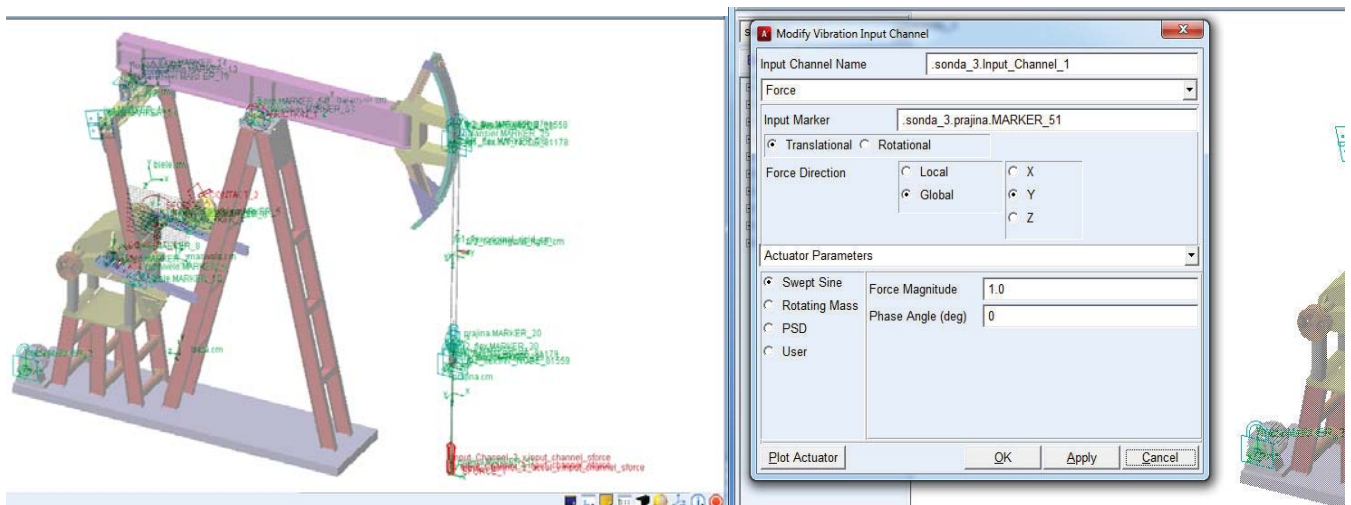


Fig. 17 Input channel definition for the force oriented on Y global axis

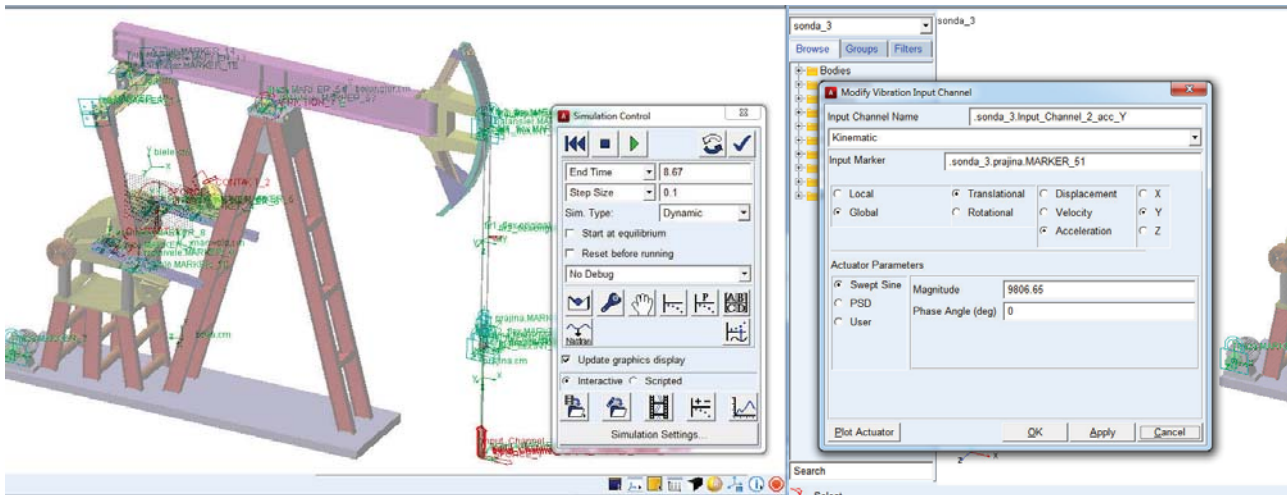


Fig. 18 Input channel definition for the acceleration on Y global axis

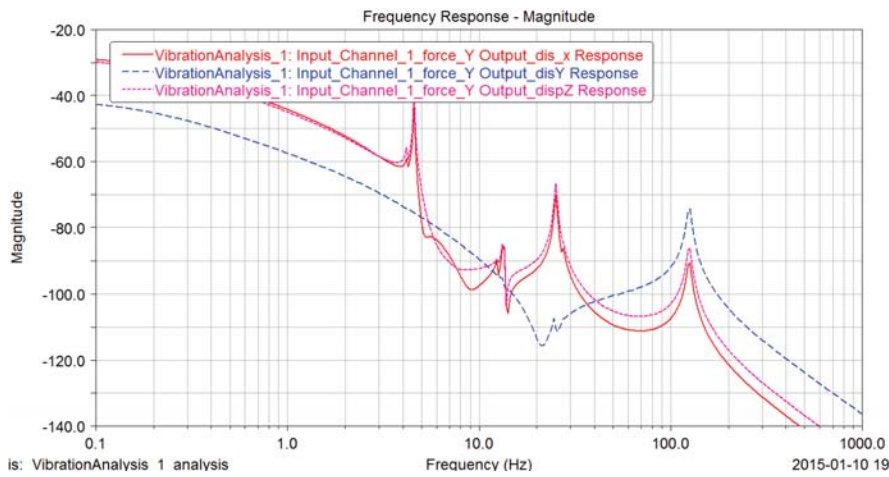


Fig. 19 Frequency response comparative analysis for the flexible element displacement on X, Y and Z axes

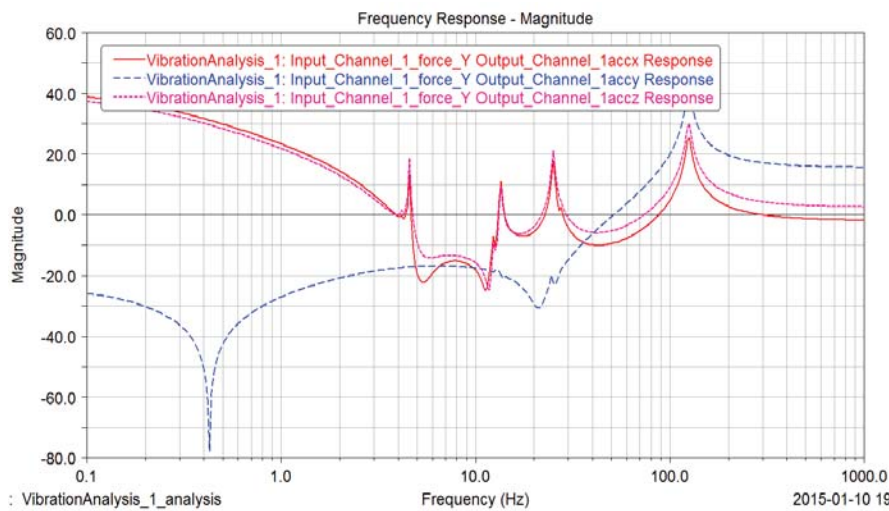


Fig. 20 Frequency response comparative analysis for the flexible element acceleration on X, Y and Z axes

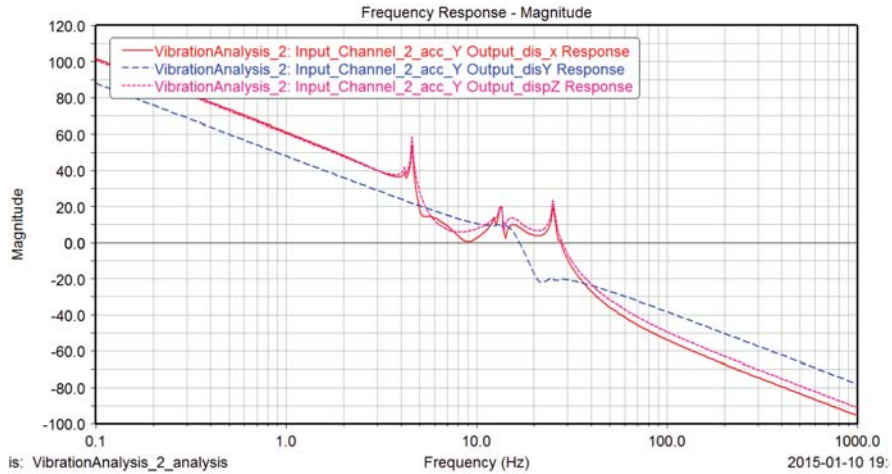


Fig. 21 Frequency response comparative analysis for flexible element center of mass displacement on X, Y and Z axes

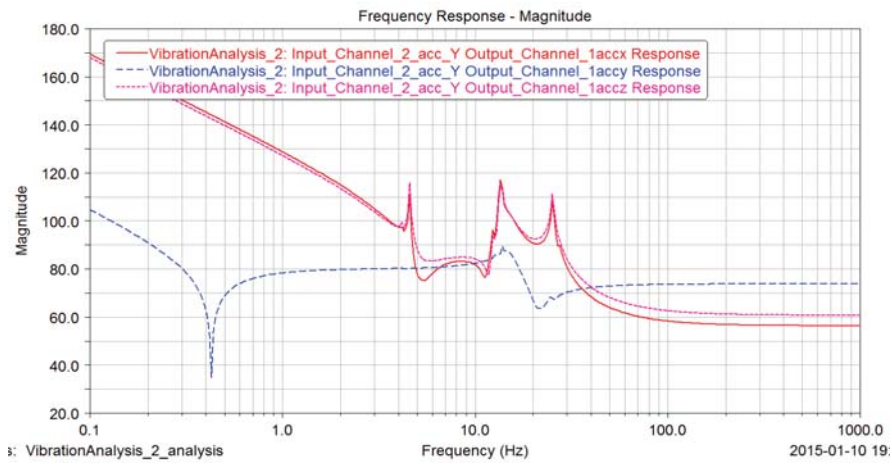


Fig. 22 Frequency response comparative analysis for flexible element center of mass accelerations on X, Y and Z axes

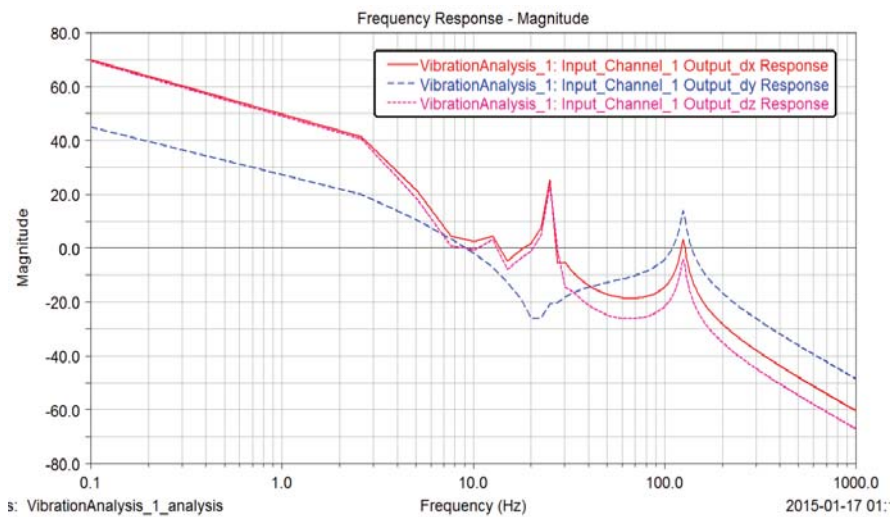


Fig. 23 Frequency response analysis for linear displacements under X, Y and Z axes of the walking beam mass

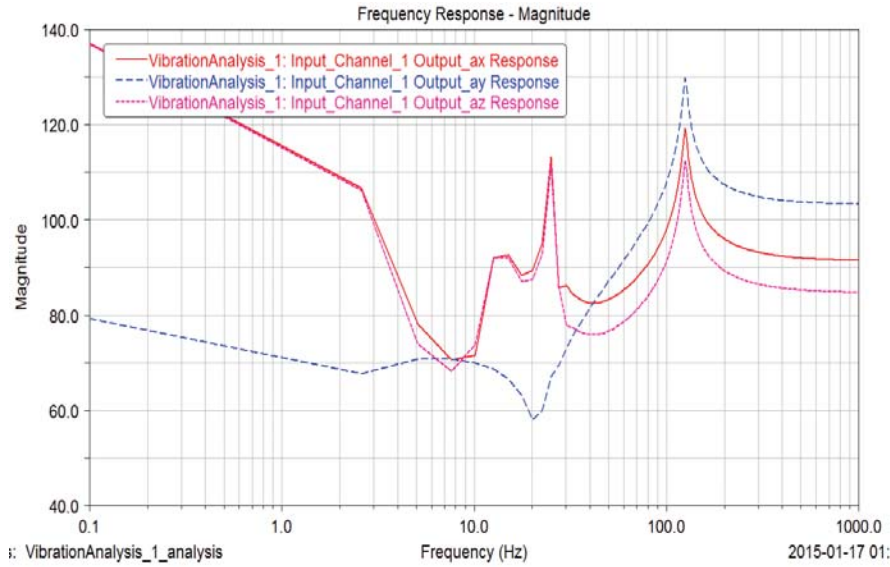


Fig. 24 Frequency response analysis for linear accelerations under X, Y and Z axes of the walking beam mass

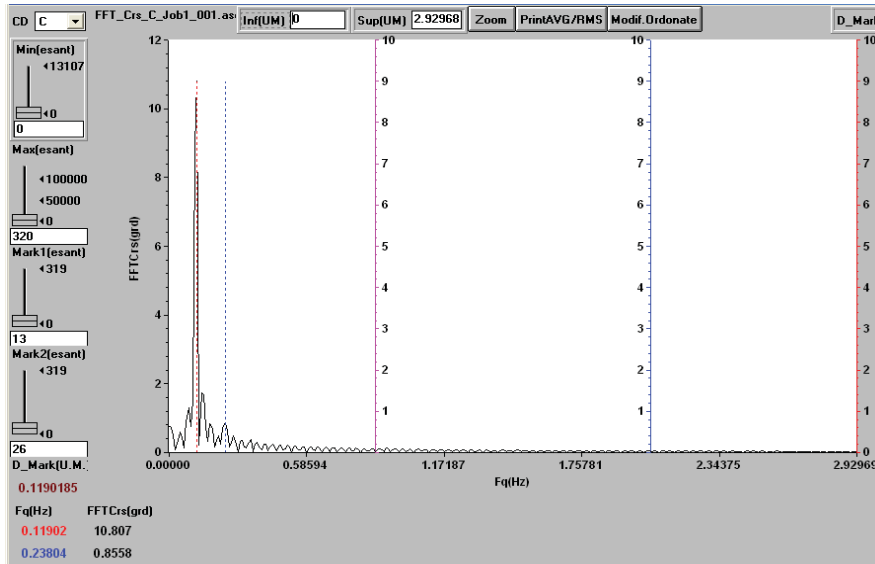


Fig. 25 Response spectrum in frequency domain of the walking beam rotation

It is very important that the forced vibrations analysis for the case when the actuator was defined as the stiffness force which was established on experimental way from Fig. 7. Thus, the following input channels were defined: force on Y global axis (Fig. 17), which was redirected on the polished rod, and acceleration on Y global axis of the polished rod no. 4 as it can be seen on Fig. 18. Through this analysis, the frequency response will be studied for the flexible element, by taking into account the mass center of this, respectively linear displacements, speeds and accelerations and even angular ones. The obtained numerical results are represented through plots which are shown in Figs. 19-24.

From the plots, a comparative study of the flexible element displacements on x, y, and z axes for a frequency domain of 100 Hz can be remarked. On this domain, there were recorded maximum values for the displacements around 4 Hertz, 12

Hertz and 100 Hertz. Similarly, there were recorded maximum values in case of accelerations, with an important remark onto obtaining high values for amplitudes on Z axis. This axis emphasizes the flexible element transversal motion.

When the actuator was considered as the acceleration parameter on global Y axis, flexible element displacement maximum values were recorded around 4 Hertz, 10 Hertz and 12 Hertz, as it can be observed on plots from Fig. 20.

By analyzing Figs. 21 and 22, it can be observed that the linear and angular accelerations reach highest values around fundamental frequency of 0.168 Hertz.

In Figs. 23 and 24, a comparative analysis of the frequency response for the walking beam mass center is presented. From these it can be remarked two critical points around 11.5 Hertz and 100 Hertz (Fig. 23). For the walking beam accelerations, there were identified three critical points of 8 Hertz, 11.5

Hertz, and 100 Hertz.

IV. FREQUENCY EXPERIMENTAL ANALYSIS

Frequency experimental analysis was performed after selecting a number of complete functionality cycles of the oil pump mechanism. The length of the recorded data was set to 188522 samples. In case of frequency domain, this was set to 262144 samples. The proper resolution in accordance with the total number of samples was set to 0.009155 Hertz. During experimental analysis, the following parameters were analyzed: T_b (MPa) – mechanical stress from the walking beam; T_p (MPa) – mechanical stress from the calibrated polished rod; A_p (m/s²) – vibration acceleration of the walking beam; A_b (m/s²) – vibration acceleration of the calibrated

polished rod; Crs (grd) – the walking beam angular displacement. Thus, in Fig. 25, a first set of the desired parameters were recorded and it can be remarked that in response spectrum exists only a fundamental harmonic with frequency equal to the work one of 0.119Hertz. In this case, the harmonic of rank 1 is neglected due his small value of 0.238 which represents around 7.9% from the fundamental one.

From Fig. 26, it can be observed that the mechanical stress and accelerations have two zones with a high frequency response, respectively the first one it is located around of fundamental frequency zone, and other is on the frequency band of 12 – 13 Hertz.

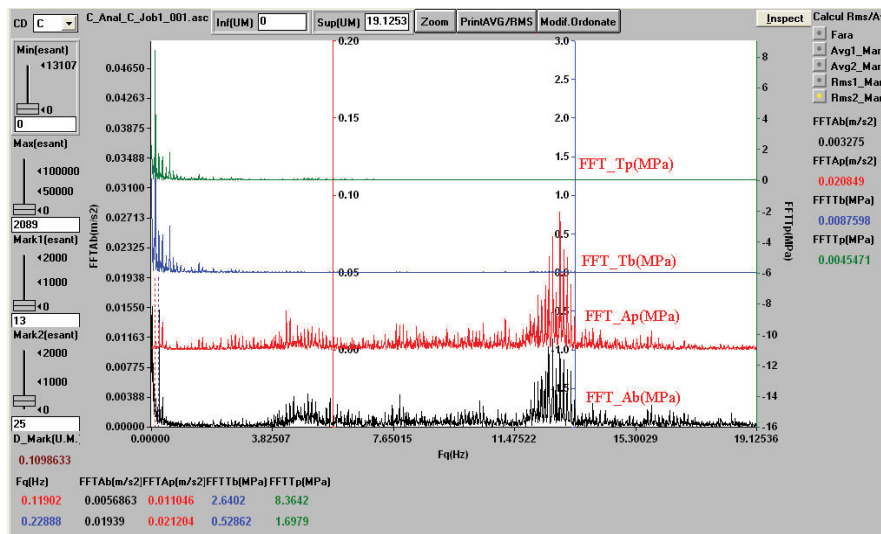


Fig. 26 Response spectrum in frequency domain for mechanical stress and accelerations

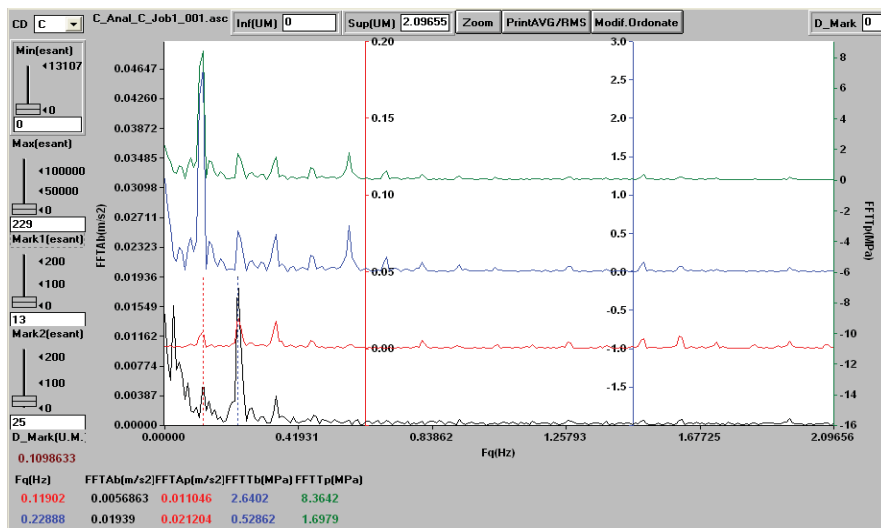


Fig. 27 A detailed view of the response frequency spectrum of the mechanical stress and accelerations

A detailed view is shown in Fig. 27 and in Table I, spectral harmonic amplitudes are given for mechanical stress and accelerations. By analyzing the obtained data from Table I, the

presence of the harmonic of 1, 2, 3, 4 ranks can be remarked which have a lowest amplitude. The accelerations have a maximum response on the first harmonic, due to the fact that

on one functional cycle both valves from the oil pump unit are actuated in case of ascendant course but also on descendent one. Also, the harmonic amplitudes values from the calibrated polished rod are doubled, by comparing these with the harmonic values of the walking beam accelerations. Considering these conditions, a spectral analysis of the calibrated polished rod superior part, namely $A_p(m/s^2)$, on a complete functional cycle presented on Figs. 28 and 29 will be

performed. For this, an area which corresponds to the descendent course of the polished rod when an oil pressure was low inside on the oil down hole pump was selected. In this way, there is no overpressure resulted by the pumping and the inertia force which actuates on the oil down hole pump is oriented in an opposite way of the piston displacement. For this descendent course, the obtained results are shown in Fig. 30 with a proper frequency spectrum in Fig. 31.

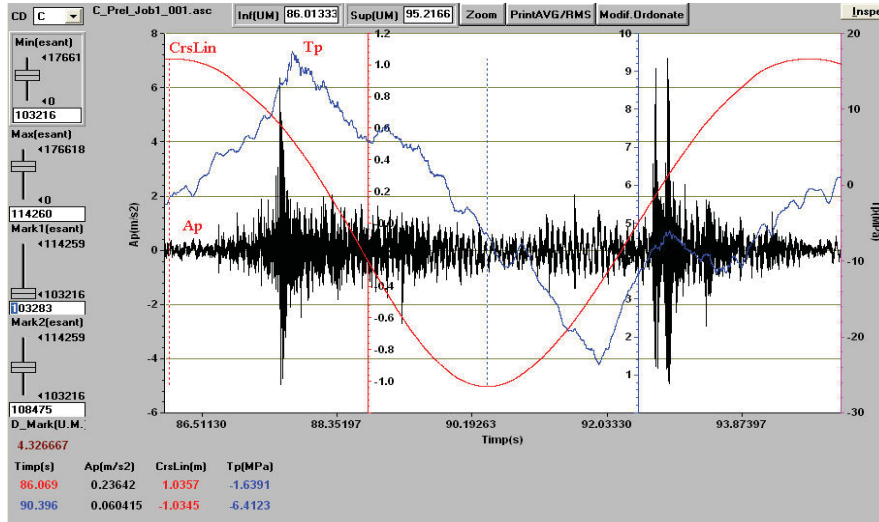


Fig. 28 A complete functional cycle for performing a spectral analysis

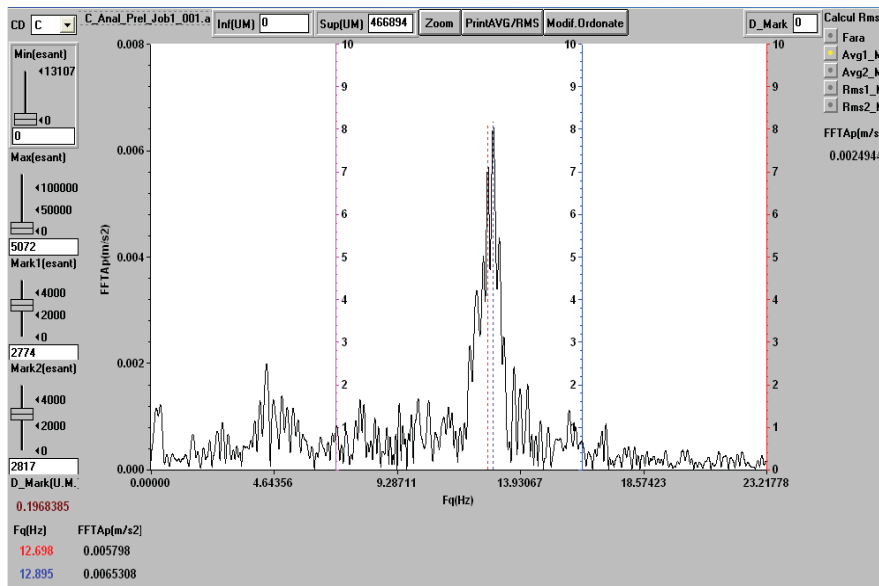


Fig. 29 A detailed view of the spectral analysis for a complete functional cycle

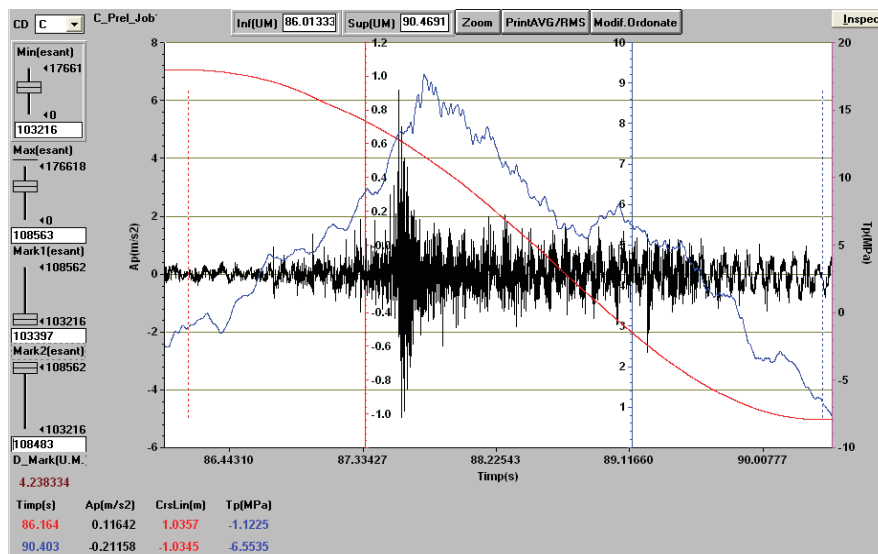


Fig. 30 One functional cycle for the descendent course

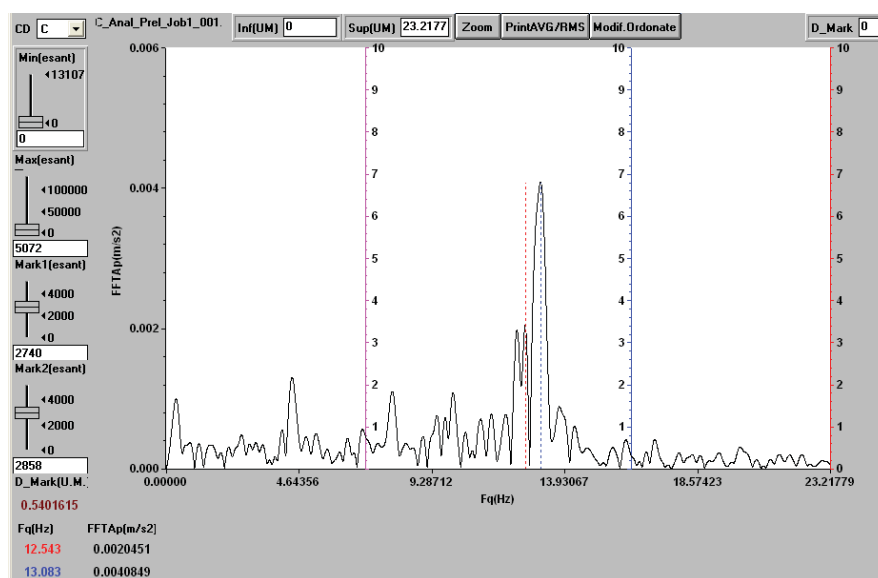


Fig. 31 Proper spectral analysis for the descendent course

TABLE I
 SPECTRAL HARMONICS AMPLITUDES FOR MECHANICAL STRESS AND ACCELERATIONS

Harmonic	Fq (Hz)	FFTA _b (m/s ²)	FFTA _p (m/s ²)	FFTT _b (MPa)	FFTT _p (MPa)
0	0.119	0.005686	0.011046	2.640181	8.364207
1	0.2288	0.01939	0.021204	0.528623	1.697903
2	0.3479	0.003808	0.017766	0.488988	1.465655

From Fig. 31, an area was selected when on oil pumping down hole a high oil pressure is exercised due to the pumping effect but also to the inertia effect of the oil inside of the oil pipe lines. This is represented in Fig. 32, and in Fig. 33, there is shown the proper frequency spectrum.

The obtained results are presented in Table II, and these were identified as the spectral lines amplitudes of the vibration

acceleration from the superior part of the calibrated polished rod. These were obtained on the frequency domain of 12 – 13 Hertz, for all the analyzed cases previously presented.

From the analysis of Figs. 31-33, it can be observed that the spectral line of a complete cycle represents the sum of all partial spectral lines for both courses. This can be remarked also on Table II. By tearing apart the spectral lines, in reality this was caused by the fact that the elastic system consists of three elastic sub systems for dynamic interaction, namely: steel cable, tubing, and polished rod.

The polished rod proper frequency according with the descendent course was 13.083 Hertz and for the ascendant course, this was 12.271 Hertz. From these values, it can be remarked that during on ascendant course, inertia forces are present and actuate on opposite direction.

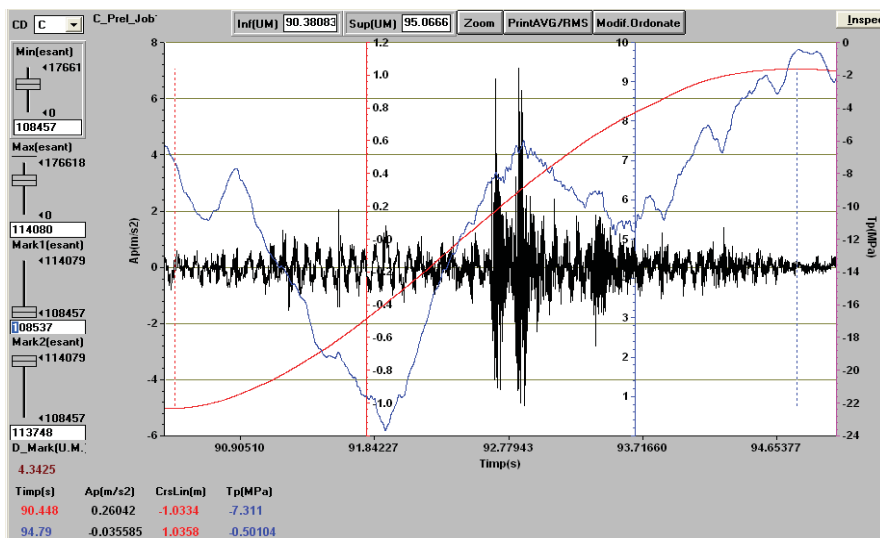


Fig. 32 One functional cycle for the ascendant course

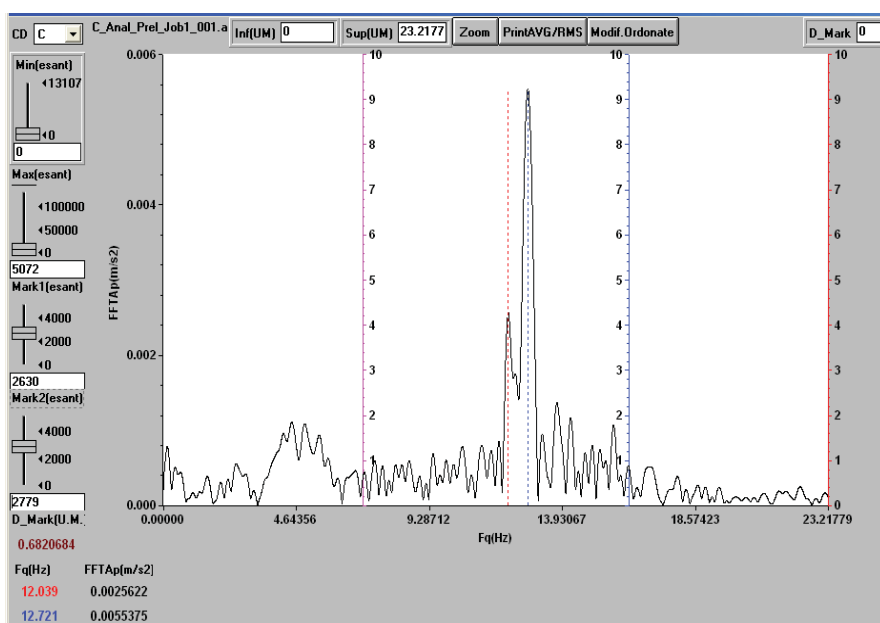


Fig. 33 Proper spectral analysis for the ascendant course

TABLE II
 SPECTRAL LINES AMPLITUDES OF POLISHED ROD ACCELERATIONS IN CASE
 OF A STABILIZED PUMPING FUNCTIONAL CYCLE

Complete cycle		Descendent course		Ascendant course	
Fq (Hz)	FFTAp (m/s ²)	Fq (Hz)	FFTAp (m/s ²)	Fq (Hz)	FFTAp (m/s ²)
12.0208	0.0023	-	-	12.039	0.002562
12.272	0.0033	12.254	0.0019	12.281	0.001752
12.529	0.0040	12.542	0.00204	-	-
12.698	0.0057	-	-	12.721	0.005538
12.895	0.0065	-	-	-	-
13.128	0.0043	13.082	0.0040	-	-

The proper frequency displacement is for all three frequencies and corresponds with the global elastic system of polished rod – tubing – down hole pump.

From the experimental tests, important information

regarding the pumping unit dynamics and the main sources that could be cause damage the oil pumping mechanism can be obtained. In addition, this analysis confirms that the mechanism flywheel is well dimensioned; otherwise this could be damaged the calibrated polish rod.

In case of the $A_b(m/s^2)$ walking beam accelerations, and the $A_p(m/s^2)$, which corresponds to the superior part of the polished rod, a maximum frequency response was obtained on the first harmonic. If it will refer to the frequency spectrum domain, the fundamental frequency has low amplitude on the second harmonic. Thus, the acceleration harmonics amplitudes of the analyzed calibrated polished rod are doubled by comparing with the walking beam transversal acceleration harmonics.

From the spectral analysis of the polished rod accelerations,

namely $A_p(m/s^2)$, it can be highlighted that for one complete functional cycle of the calibrated polished rod, the vibrations from the down hole pump have different spectral characteristics for both cycle phases. The elastic system formed from steel cable – polished rod – tubing behaves like an elastic system coupled through damping (viscous damping of the oil tubing). The resonance frequencies for this system are in the frequency domain of 12 – 13 Hertz for each component according with his proper spectral line.

The proper frequencies, for the mentioned elastic system in case of the ascendant course, are lower than others from descendent course. This is caused by the oil quantity which was pumped from down hole. In this case, the inertia forces are higher on the opposite way of the piston displacement. The proper frequency in this case for the polished rod is situated at a value of 12.721Hertz for ascendant course and in case of descendent course this has a value of 13.083Hertz.

Through this experimental analysis, it results that the proper frequencies displacement in case of the polished rod are in a straight connection with the loading level of the oil pump unit.

If the oil pump unit will work at high capacity, this will increase the oil pressure from the pumping tubes and the proper frequencies of the polished rod will be low. In this case, the oil pumping unit will work in poor conditions due to the low frequencies on one cycle (ascendant/descendent phases) and it can be remarked a displacement to the high frequencies over the proper polished rod proper frequencies.

V. CONCLUSIONS

Through this research, an oil pump unit was analyzed. A special attention was given to the vibration measurements and analyses of the oil pump mechanism and also to the vibration sources identification.

The experimental results were also verified with the ones from a modal analysis by using finite element method. The obtained vibrations give essential information for the technical data evaluation of the analyzed mechanism.

There were performed numerical simulations on dynamic mode for different motion torque variation laws and also for angular speeds which the recorded outputs were emphasized on kinematic parameters variation, namely for the deformable solid motion of the elastic cable.

The vibrations experimental analysis performed in a period of time and also in frequency domain was completed with a modal dynamic analysis achieved with finite element method.

From the experimental tests, the polished rod is the most exposed element to accidents due to its brake risk, and in case of an overload, this could brake by taking into account the material fatigue.

REFERENCES

[1] D.G. Beale, S.W. Lee, "A mode method for an elastic rod in a fluid pumping system", *Journal of Sound and Vibration*, 179(1), 1995 Academic Press Limited, pp. 97-108.
[2] B. Ramkamal, A. Fashesan, R. Heinze, F. Lea, "A Computational Method for Planar Kinematic Analysis of Beam Pumping Units", *Journal of Energy Resources Technology*, Volume 129, Issue 4, 300 (7 pages). 2007

[3] C. Yibao, L. Jianfu, "Optimum design of four-bar linkage of beam-pumping unit based on sensitivity analysis", *2010 International Conference on Logistics Systems and Intelligent Management*.
[4] X. Y. Gang, S. F. Wang, Y. Han, "An Explicit Analysis Method for Walking-Beam Oil Pumping Unit", *Applied Mechanics and Materials Journal* (Volumes 26 - 28), 2010.
[5] X. Liu, Y. Qi, Y. Li, C. Liu, "An Approach to the Design Calculation of Sucker Rod Pumping Systems in Coal bed Methane Wells", *Chinese Journal of Mechanical Engineering*, Vol. 24, DOI: 10.3901/CJME.2011.
[6] J. C. Ng, S. Dubljevic, "Dynamical Analysis of Sucker-Rod String" *Artificial Lift Systems for Control Applications, Annual Meeting, Computing and Systems Technology Division*, 2011.
[7] Yu Yang, J. Watson, S. Dubljevic, "Modeling and Dynamical Analysis of the Wave Equation of Sucker-Rod Pumping System", *SPE Annual Technical Conference and Exhibition, USA*, published by Society of Petroleum Engineers, 2012.
[8] L. S. Firu, T. Chelu, C. Militaru-Petre, "A Modern Approach to the Optimum Design of Sucker-Rod Pumping System", *SPE Annual Technical Conference and Exhibition, USA, Colorado*, 2003.
[9] H. S. Luiz Torres, L. Schmitman, "Modelling and Identification of a Sucker-Rod Pumping System of Oil Wells", *Recent Advances in Mathematical Methods, Intelligent Systems and Materials, Proceedings of the 15th International Conference on Mathematical Methods, Computational Techniques and Intelligent Systems (MAMECTIS '13), Proceedings of the 6th International Conference on Materials Science (MATERIALS '13)*, Cyprus, 2013.
[10] X. Zhang, X. Yang, Z. Guo, "Kinematics and Dynamics Analysis of Drive Mechanism of Parallel Four-Bar Energy-Saving Pumping Unit", *Journal of Natural Sciences*, 2012, Vol.17 No.1, pp. 073-078.
[11] G. Takacs, "Sucker-Rod Pumping Manual", Penn-Well Books, Tulsa, USA, 2002.
[12] R.R. Craig and M.C.C. Bampton. Coupling of substructures for dynamics analyses. *AIAA Journal*, 6(7), pp. 1313-1319, 1968.
[13] N. Dumitru, N. Craciunoiu, R. Malciu N. Ploscaru, "Elastodynamic analysis of a Beam Pumping Unit Mechanism", *International Conference of Mechanical Engineering. ICOM-2013, Craiova-Romania*, Vol. 1, pp. 27-36.